AGU PUBLICATIONS

Geophysical Research Letters

RESEARCH LETTER
10.1002/2013GL058789

Key Points:
- Long-duration isolated-like ejecta at 1 AU may result from multiple CMEs
- Such events may drive the magnetosphere for long periods with sawtooth events
- In situ measurements may be misleading, and propagation must be accounted for

Correspondence to:
N. Lugaz,
noe.lugaz@unh.edu

Citation:
Lugaz, N., and C. J. Farrugia (2014), A new class of complex ejecta resulting from the interaction of two CMEs and its expected geoeffectiveness, *Geophys. Res. Lett.*, *41*, 769–776, doi:10.1002/2013GL058789.

Received 21 NOV 2013
Accepted 14 JAN 2014
Accepted article online 20 JAN 2014
Published online 11 FEB 2014

A new class of complex ejecta resulting from the interaction of two CMEs and its expected geoeffectiveness

N. Lugaz[1] and C. J. Farrugia[1]

[1]Department of Physics and Space Science Center, University of New Hampshire, Durham, New Hampshire, USA

Abstract A significant portion of transients measured by spacecraft at 1 AU does not show the well-defined properties of magnetic clouds (MCs). Here we propose a new class of complex, non-MC ejecta resulting from the interaction of two coronal mass ejections (CMEs) with different orientations, which differ from previously studied multiple-MC events. At 1 AU, they are associated with a smooth rotation of the magnetic field vector over an extended duration and do not exhibit clear signs of interaction. We determine the characteristics of such events based on a numerical simulation and identify and analyze a potential case in the long-duration transient event measured in situ on 19–22 March 2001. Such events may result in intense, long-duration geomagnetic storms, with a sequence sawtooth events, and may sometimes be misidentified as isolated CMEs.

1. Introduction

Coronal mass ejections (CMEs) are the major driver of intense geomagnetic activity [*Richardson et al.*, 2001] and have been studied extensively for the past 40 years. CMEs are observed remotely by coronagraphs and heliospheric imagers and measured in situ by spacecraft such as ACE and Wind. Since the launch of SOHO and STEREO, the availability of white light imagers with wide fields of view has made it possible to associate eruptions observed in the corona to CMEs measured in situ at 1 AU (see, for example, the list by *Richardson and Cane* [2010]). CMEs measured in situ may be divided into three broad categories: magnetic clouds (MCs), non-MC isolated ejecta, and complex ejecta (similar to the categories of *Zurbuchen and Richardson* [2006]). MCs have well-defined properties [see *Burlaga et al.*, 1981]. Non-MC isolated ejecta typically have some but not all the properties of MCs and are sometimes referred to as MC-like ejecta [*Lepping et al.*, 2005; *Al-Haddad et al.*, 2013]. They may correspond to a distorted CME or to the crossing through the "leg" of a CME. Lists of MCs and MC-like ejecta measured at 1 AU by the Wind and ACE spacecraft are maintained [*Lepping et al.*, 2005; *Jian et al.*, 2006; *Richardson and Cane*, 2010].

Complex ejecta result from the interaction of successive CMEs [*Burlaga et al.*, 1987]. Some consist of many individual eruptions, and it is then impossible to relate in situ measurements to coronagraphic observations of CMEs [*Burlaga et al.*, 2002]. Others are made up of two clearly distinct MCs separated by an interaction region (multiple-MC events, see *Wang et al.* [2003] and *Lugaz et al.* [2005]). Complex ejecta tend to have long durations and may drive the magnetosphere for an extended period. *Xie et al.* [2006], for example, studied long (≥3 days) and intense ($Dst_{peak} \leq -100$ nT) geomagnetic storms and found that 24 out of 37 such storms were associated with multiple CMEs (also *Farrugia et al.* [2006]).

While a typical CME passes over Earth in ~ 20 h, some events last well in excess of 30 h [*Marubashi and Lepping*, 2007]. It is possible that some of these long-duration events, believed to be associated with a single, isolated CME, are in fact the results of the interaction of two CMEs, a possibility raised for a specific CME (15 May 2005) by *Dasso et al.* [2009].

Here we identify a new type of complex ejecta arising from the interaction of two CMEs, which results in a long-duration event with a smooth rotation of the magnetic field vector. In section 2, we present the result at 1 AU of two simulations, one of an isolated CME, and one of two interacting CMEs. In section 3, we first discuss the expected geoeffectiveness of such events in general terms and then analyze the in situ measurements of the 19–22 March 2001 period, which may be associated with the interaction of two CMEs in a way similar to that of the simulation. We discuss our findings and conclude in section 4.

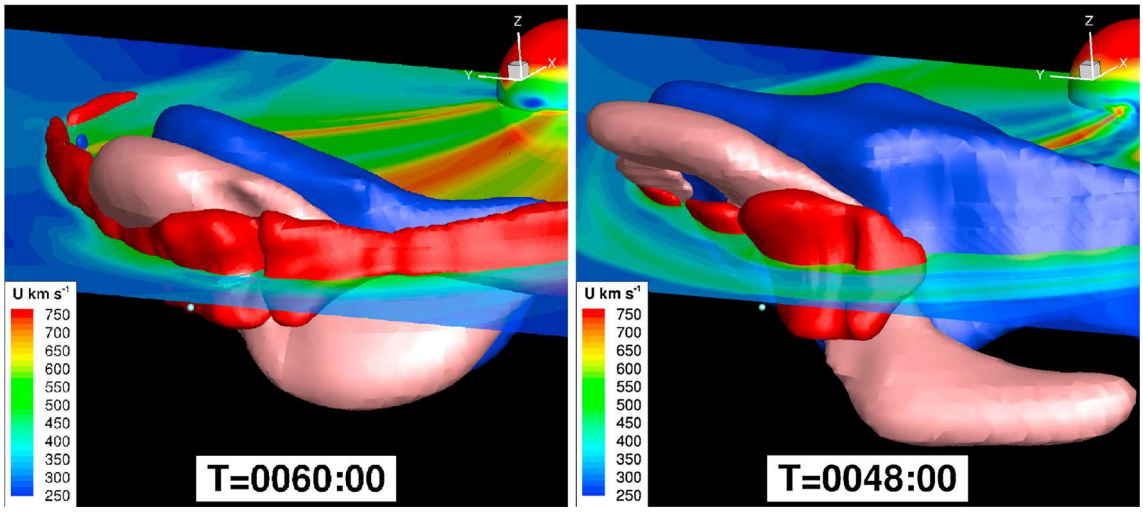

Figure 1. (left) Simulation result at hour 60 corresponding to isolated CME1. The pink isosurface corresponds to values of $B_y = 20$ nT; the red and blue isosurfaces correspond to values of $B_z = \pm 20$ nT, respectively. The sphere of radius 20 $R_\odot$ centered at the Sun's position and the cut in the ecliptic plane are color coded with the velocity. (right) Simulation result at hour 48 corresponding to the two interacting CMEs with the same conventions as the image of Figure 1.

2. Simulated Magnetic Cloud and Complex Ejecta

2.1. Simulation Setup

The simulation setup is in nearly identical to that of *Lugaz et al.* [2013] for their Case C (two CMEs with orientation 90° apart). We summarize the important details here as well as one difference with this previous simulation and refer the interested reader to this paper for further information. We use the Space Weather Modeling Framework [*Tóth et al.*, 2012] to perform the simulations. The simulation domain is a Cartesian box centered at the Sun and extending to ± 220 $R_\odot$ in all three directions. The domain is resolved with a maximum of 34 million cells ranging in size from 0.01 to 4 $R_\odot$ after adaptive mesh refinement. Along the Sun-Earth line, cell size of 0.05 $R_\odot$ is maintained up to 0.4 AU (0.1 $R_\odot$ resolution afterward).

We use the solar wind model of *van der Holst et al.* [2010] where Alfvén waves drive the solar wind. To set up the solar magnetic field, we use a nontilted dipole with an octopole component, which yields a maximum magnetic field strength of 5.5 G at the solar poles with a polarity corresponding to that of solar cycle 24. To initiate the CMEs, we insert right-handed flux ropes using the model of *Gibson and Low* [1998] (GL) in a state of force imbalance onto the steady state solar corona. The parameters of the GL flux rope for the two CMEs are the same as for the Case C from *Lugaz et al.* [2013], the only difference being the time delay between the two CMEs, which is 15 h instead of 7 h. The first CME (CME1) has a low inclination and an eastward axial field: a NES cloud according to the categorization of *Bothmer and Schwenn* [1998]. The second CME (CME2) is highly inclined with a southward axial field: a ESW cloud. For comparison purposes, we also perform the simulation of an isolated event by simply propagating the CME1 all the way to 1 AU without the second eruption. The simulation setup is purposely kept idealized. CME propagation is known to be strongly affected by their interaction with the ambient solar wind [e.g., see *Manchester et al.*, 2004; *Savani et al.*, 2010]. While simulations of real instances of CME-CME interaction have been performed before [*Lugaz et al.*, 2007; *Shen et al.*, 2011], here we choose to use an idealized and axisymmetric magnetic field and solar wind background to focus on the effects of the CME-CME interaction.

2.2. Simulated Magnetic Cloud at 1 AU

Three-dimensional results of the isolated CME simulation are shown in Figure 1 (left) with isosurfaces of magnetic field equals to 20 nT highlighting the CME. The magnetic ejecta has a reverse-S shape, characteristic of the GL model [see *Gibson and Low*, 1998; *Manchester et al.*, 2004]. Synthetic spacecraft measurements at 1 AU are shown in Figure 2 (left). It corresponds to a moderately fast CME with a transit time of about 63 h for the shock and 70 h for the magnetic ejecta. The CME has a speed at 1 AU of about 540 km s^{-1} and is characterized by a NES rotation. The sheath duration is about 7 h, and the magnetic ejecta lasts for about 23 h, corresponding to a width of ~0.28 AU.

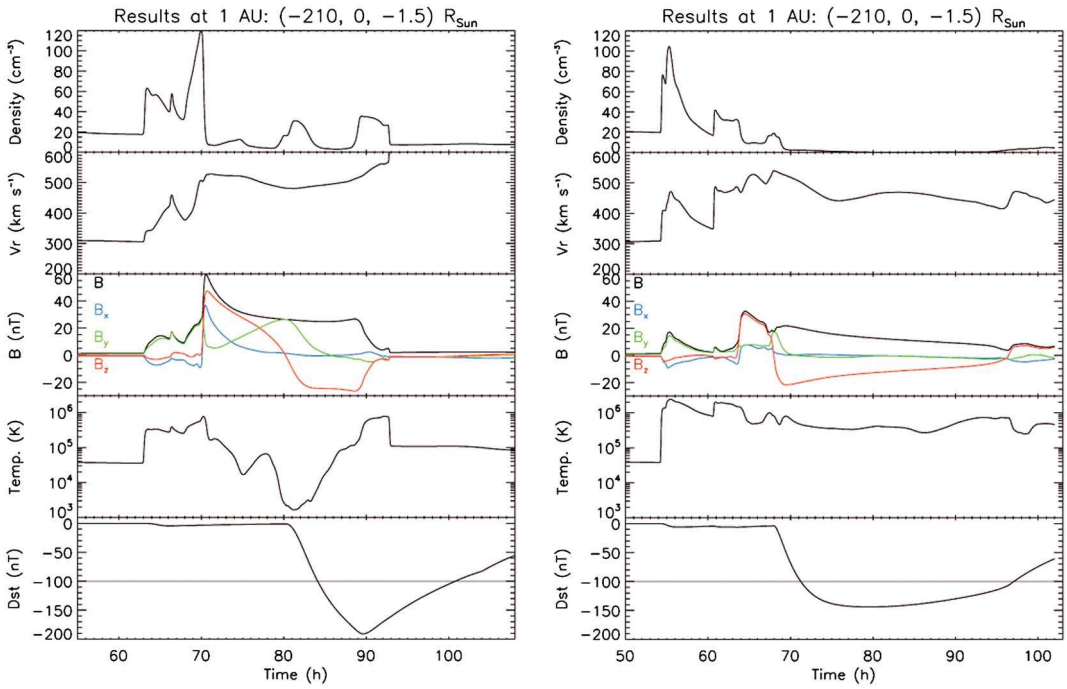

Figure 2. (left) Simulation result at 1 AU of an isolated CME and modeled *Dst* index. (right) Simulation result at 1 AU of a complex ejecta corresponding to the two interacting CMEs described in the text. (top to bottom) The density, radial velocity, magnetic field, temperature, and derived *Dst* with the same scales.

2.3. Simulated Complex Ejecta at 1 AU

Next, we discuss the results of the simulation for the two interacting CMEs. The timing of the interaction goes as follows: the shock driven by CME2 reaches the back of CME1 at hour 18.5, its center at hour 22.5 and the back of the sheath at hour 24. At hour 29, the two shocks have merged and reached a distance of 0.47 AU from the Sun. The results at hour 48, as the complex ejecta is close to 1 AU, are shown in Figure 1 (right). At the back of CME1, there is an extended period of southward magnetic field, as is clear from the large blue isosurface in Figure 1.

Synthetic spacecraft measurements at 1 AU are shown in Figure 2 (right). A single fast-mode shock at hour 54 precedes the complex ejecta, which starts at hour 63. The complex ejecta is characterized by a relatively short period of northward B_z lasting about 5 h and an extended "tail" of southward B_z for about 28 h. The east-west component of the magnetic field, B_y, is close to zero for the last 24 h of the event, after an initial period of eastward magnetic field. Throughout the complex ejecta, the velocity profile is decreasing from about 540 to 450 km s^{-1}.

The main differences between the isolated MC and the complex ejecta resulting from the interaction of two CMEs are the following: (i) shorter transit time of the complex ejecta as compared to the isolated CME, (ii) short duration of the first CME (here about 8 h versus 28 h for the isolated one), and (iii) hotter and somewhat denser sheath region preceding the complex ejecta.

3. Geoeffective Potential of Complex Ejecta

3.1. Simulated Events

We estimate the *Dst* corrected for the contribution of the ram pressure, *Dst**, from the simulated in situ measurements using a modified version of the *Burton et al.* [1975] relation: $\frac{d}{dt}\,Dst^* = Q(t) - Dst^*/\tau$, with $Q = -1.22 \times 10^{-3}\left(VB_z - 0.49\right)$ if $VB_z > 0.49$ mV m^{-1}, and Q = 0 otherwise, and with $\tau = 8.64 \times 10^3 \exp\left(9.74/(4.69 + VB_z)\right)$ if $B_z < 0$ nT and $\tau = 3.57 \times 10^4$ otherwise.

The results are shown in Figure 2 (bottom). Both the isolated CME and the complex ejecta would have resulted in an intense geomagnetic storm with a peak *Dst* below −100 nT. The isolated CME results in a

relatively typical intense geomagnetic storm with a main phase lasting about 9 h, a peak *Dst* of −191 nT following by a recovery phase lasting more than 1 day. The *Dst* is below −100 nT for about 16.5 h. The complex ejecta, on the other hand, results in a weaker storm with a peak *Dst* of −144 nT. The main phase lasts about 12 h and the recovery phase about 1.5 days. The *Dst* is below −100 nT for 26 h or about 55% longer than for the isolated CME. Note also that the southward magnetic field in the sheath region results in a very small negative *Dst* for the isolated and interacting CMEs around hours 65 and 55, respectively.

The larger *Dst* in the isolated CME is due to a combination of factors: the minimum southward B_z is slightly larger (−26.5 versus −21.6 nT); it occurs at the end of the southward magnetic field period instead of at its beginning and the velocity in the complex ejecta decreases faster than in the isolated CME (resulting in a smaller dawn-to-dusk electric field). However, the longer period below −100 nT predicted for this complex ejecta may result in an intensification of the geomagnetic response, which cannot be captured by our simple model to evaluate the *Dst* index.

3.2. An Observed Event

To confirm that this type of complex events indeed exists, we identify potential examples in in situ data at 1 AU. Note that *Dasso et al.* [2009] discuss a complex event which may be the result of the interaction of two successive CMEs on 15 May 2005 and appear as a long-duration isolated MC. Here we start from the list of 17 events from *Marubashi and Lepping* [2007] and that from *Xie et al.* [2006]. The complex event from 19–22 March 2001 is one of the best examples of a potential long-duration complex ejecta resulting from multiple CMEs (another candidate, not discussed here, occurred on 3–5 April 2004). Figure 3 shows the in situ measurements including the clock angle of the interplanetary magnetic field (IMF), θ. The magnetic ejecta lasts for about 57 h (between the two vertical red lines). It is preceded by a single fast-mode shock at 11:30 UT on March 19 (marked by the first vertical line). The velocity profile through the CME is similar to that of an isolated expanding event: monotonically decreasing with a center value of 400 km s^{-1} and a radial expansion speed of 100 km s^{-1}. The magnetic field strength is very smooth and reaches a maximum of $\sim$ 22 nT, and the plasma β is well below 0.1 throughout the structure. There are, however, some indications of an origin from two structures with an interface around 18–20 UT on 20 March: (i) the fluctuations in the magnetic field vectors occur in all three components from the start of the event to 20 UT on 20 March; thereafter, only the B_x and B_z components fluctuate, but the B_y component is smooth; (ii) the magnetic clock angle varies (first decrease to 180° then increase back to 90°) during the first part and is steady (eastward directed) afterward, and, (iii) the merging electric field, $E_{KL} = V\sqrt{B_y^2 + B_z^2}\sin^2(\theta/2)$ following *Kan and Lee* [1979] (shown in Figure 4) implies strong forcing of the magnetosphere during the first part (large values $\sim$ 5 mV/m) and decreases monotonically thereafter. Also, small-scale structures (identified as slow shocks) are present near the peak of the magnetic field strength (20 March around 18–20 UT).

All but one tabulation of MCs consider this a single event with a duration of more than 50 h [see, for example, *Jian et al.*, 2006; *Marubashi and Lepping*, 2007; *Richardson and Zhang*, 2008], about twice longer than the typical duration of a magnetic cloud at 1 AU. The exception to this interpretation is the list of *Lepping et al.* [2005], which identifies two overlapping MCs (the second MC starts 0.5 h before the end of the first one at 17:45 UT on 20 March). We performed a minimum variance analysis on the magnetic field for the two separate intervals. Both returned a robust result (ratio of intermediate-to-minimum eigenvalues > 4) and yielded two inclined clouds with an angle of $\sim$ 40° between them.

This event resulted in a double-peaked intense geomagnetic storm with *Dst* below −50 nT for 55 h starting on 19 March at 18 UT. The first dip of −105 nT occurred at 22 UT on 19 March and corresponds to southward IMF in the sheath preceding the magnetic ejecta. The second peak of −149 nT at 14 UT on 20 March is associated with southward IMF during the first time interval. Figure 4 shows geomagnetic indices (*AL* and *SYM* − *H*) and the energetic particle fluxes at geostationary heights from GOES 8. The storm main phase starts when the sheath is passing over the magnetosphere. The *SYM* − *H* index then decreases nonmonotonically to its peak values. Recovery starts at the time when the second interval starts (after the maximum in *B*). In addition, this time period was associated with a sawtooth event on 20 March [*Troshichev et al.*, 2011]. Sawtooth events are typically associated with a strong driver of the magnetosphere and a southward IMF for extended periods of time [*Henderson*, 2004]. There are 10 dipolarizations associated with injection of energetic particles observed at GOES 8 during the passage of the sheath and the first interval. The average and standard deviation of the duration between individual sawteeth is 2.1 ± 0.55 h, which is typical for sawteeth. During

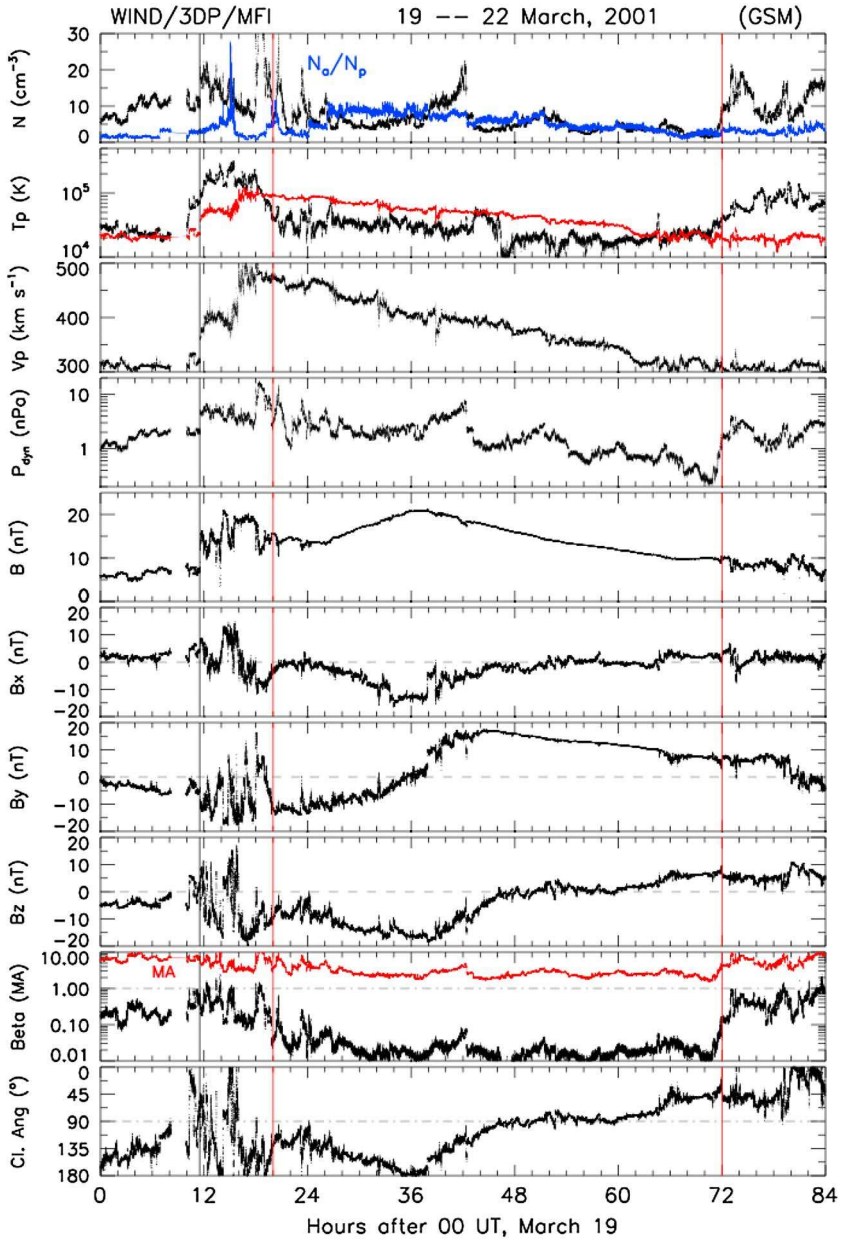

Figure 3. The 19–22 March 2001 long-duration event. (top to bottom) The proton density (alpha-to-proton ratio in blue), the proton temperature (expected temperature in red), the velocity, dynamic pressure, magnetic field strength and magnetic field vector components in GSM coordinates, the plasma β, and magnetic field clock angle, θ.

the second time interval, there are only four weak dipolarization events, none of them in the last 36 h of the event.

The ejecta measured in situ on 19–22 March 2001 is usually associated with a slow partial-halo CME observed by Large Angle and Spectrometric Coronagraph/C2 on 16 March at 03:50 UT with a speed of about 360 km s^{-1}. While the transit time to 1 AU for this CME is approximately correct, it is unlikely that such a slow CME would (i) reach speeds in excess of 500 km s^{-1} at 1 AU, as is measured here, and (ii) result in the longest MC measured during solar cycle 23 [*Marubashi and Lepping*, 2007]. On the solar side, the 14–18 March 2001 period was CME rich; there were a number of slow disk-centered eruptions on 14–15 March (for example from W10 on 15 March at 22:26 UT) as well as a full and fast halo CME on 18 March at 02:00 UT. This halo CME lacks on-disk observations and is considered back sided, but it may have been Earth directed and

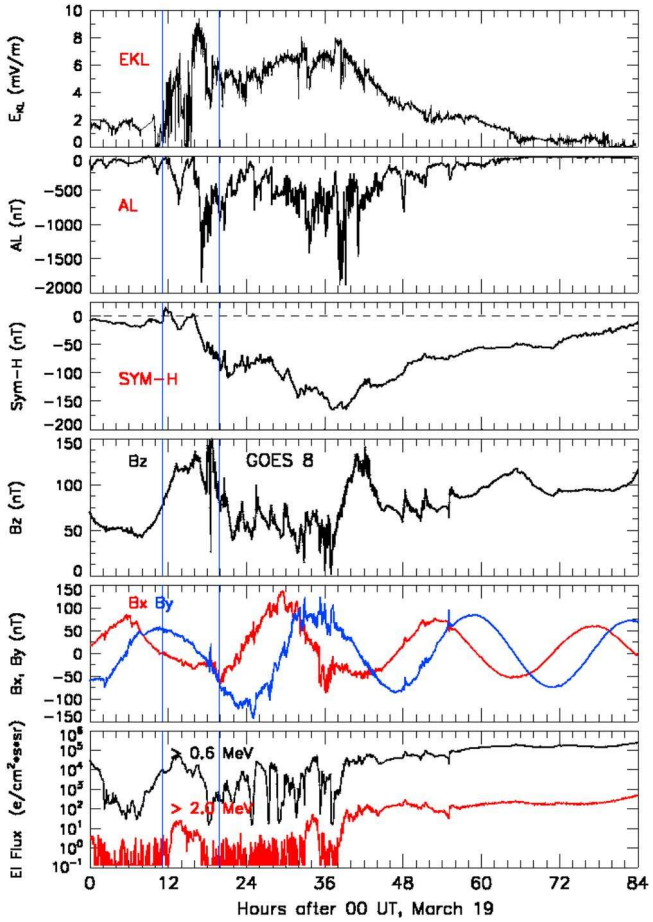

Figure 4. Geomagnetic response to the 19–22 March 2001 event. (top to bottom) The merging electric field, the *AL* and *SYM* − *H* indices, the magnetic field components and energetic particle fluxes measured by GOES 8.

could explain the origin of the second ejecta. Another more plausible possibility is that the second ejecta corresponds to a CME from W37 on 17 March at 18:00 UT which had a speed of about 600 km s^{-1}.

Overall, there are many indirect indications that this event is associated with two CMEs, contrary to what was reported by most studies. Based on the change in the rotation of the magnetic field and on the increase in proton density between 15 and 19 UT on 20 March, we can identify a first magnetic ejecta between 20 UT on 19 March and 14 UT on 20 March (18 h) and a second ejecta between 19 UT on 20 March and 00 UT on 22 March (29 h). Both ejecta have the typical duration of a MC at 1 AU. As in the simulation, the second ejecta is characterized by a smooth, enhanced and unidirectional magnetic field (for the March event in the eastward direction). In the simulation, it corresponds to the direction of the axial field of CME2 for which the poloidal field has reconnected away leaving a nearly unidirectional field. If this is the case for the March event, the second CME would be of low inclination. The lack of geoeffectiveness of this second ejecta with a strong B_y component will need to be investigated further.

4. Discussion and Conclusions

By combining numerical simulations and the analysis of in situ measurements, we have identified a new class of complex ejecta resulting from the interaction of two CMEs. Due to the different orientations of the ejections, measurements at 1 AU appear to indicate the passage of a long magnetic cloud, but are in fact, due to two successive and interacting CMEs. With an appropriate orientation of the two CMEs, such an event may result in a long-duration geomagnetic storm and a sequence of sawtooth-type substorms.

Based on a simulation of the interaction of two CMEs with different orientations, we have shown that the resulting complex ejecta is very similar to a MC from an isolated CME, except for the presence of a long "tail"

in the magnetic field and the hotter temperature throughout the ejecta. We have estimated the expected *Dst* index for this simulated complex ejecta, and we have found that while the peak *Dst* is not as low as that from a well-oriented isolated CME, the tail in the magnetic field results in the *Dst* to be below −100 nT for more than a day, or about 50% longer than for the isolated CME.

We have also presented the analysis of one long-duration magnetic ejecta observed at 1 AU on 19–22 March 2001. This event resulted in a long, intense geomagnetic storm with a peak *Dst* of −149 nT, and the *Dst* remained below −50 nT for more than 2 days. There were also a number of sawteeth on 20 March during the first half of the ejecta. Most studies have identified this time period as being associated with an isolated MC lasting more than 2 days. We have presented evidence that this ejecta is in fact a complex ejecta associated with the coalescence of two CMEs.

A more systematic investigation of combined in situ and remote sensing databases will be required to assess how common this type of complex ejecta is. This will be helped by the availability of remote sensing observations of CMEs as they propagate and interact on their way to Earth [*Shen et al.*, 2012; *Lugaz et al.*, 2012]. We have tentatively identified another event on 3–6 April 2004, which was also associated with a sawtooth event, although the *Dst* index, which peaked at −117 nT, was below −50 nT for only 15 h. Follow-up investigations will need to determine how the presence of solar wind streams may affect the formation of such complex ejecta [*Rouillard et al.*, 2010]. Further studies are also required to determine how this type of complex ejecta affects Earth's magnetosphere and how the interaction differs from that with an isolated MC or a multiple-MC event.

Acknowledgments
The research for this manuscript was supported by the following grants: NSF AGS-1239699, NASA NNX13AH94G, and NNX13AP39. The simulations were performed on the NASA HEC *Pleiades* system under award SMD-13-3919. N.L. wishes to thank the reviewer for useful comments.

The Editor thanks Ofer Cohen for his assistance in evaluating this paper.

References

Al-Haddad, N., T. Nieves-Chinchilla, C. Möstl, M. A. Hidalgo, K. Marubashi, M. P. Savani, I. I. Roussev, S. Poedts, and C. J. Farrugia (2013), Magnetic field configuration models and reconstruction methods for ICMEs: A comparative study, *Sol. Phys.*, *284*, 129–149.

Bothmer, V., and R. Schwenn (1998), The structure and origin of magnetic clouds in the solar wind, *Ann. Geophys.*, *16*, 1–24.

Burlaga, L., E. Sittler, F. Mariani, and R. Schwenn (1981), Magnetic loop behind an interplanetary shock: Voyager, Helios, and IMP 8 observations, *J. Geophys. Res.*, *86*, 6673–6684.

Burlaga, L. F., K. W. Behannon, and L. W. Klein (1987), Compound streams, magnetic clouds, and major geomagnetic storms, *J. Geophys. Res.*, *92*, 5725–5734.

Burlaga, L. F., S. P. Plunkett, and O. C. St. Cyr (2002), Successive CMEs and complex ejecta, *J. Geophys. Res.*, *107*(A10), 1266, doi:10.1029/2001JA000255.

Burton, R. K., R. L. McPherron, and C. T. Russell (1975), An empirical relationship between interplanetary conditions and Dst, *J. Geophys. Res.*, *80*, 4204–4214.

Dasso, S., et al. (2009), Linking two consecutive nonmerging magnetic clouds with their solar sources, *J. Geophys. Res.*, *114*, A02109, doi:10.1029/2008JA013102.

Farrugia, C. J., H. Matsui, H. Kucharek, V. K. Jordanova, R. B. Torbert, K. W. Ogilvie, D. B. Berdichevsky, C. W. Smith, and R. Skoug (2006), Survey of intense Sun-Earth connection events (1995–2003), *Adv. Space Res.*, *38*, 498–502.

Gibson, S. E., and B. C. Low (1998), A time-dependent three-dimensional magnetohydrodynamic model of the coronal mass ejection, *Astrophys. J.*, *493*, 460–473.

Henderson, M. G. (2004), The May 2–3, 1986 CDAW-9C interval: A sawtooth event, *Geophys. Res. Lett.*, *31*, L11804, doi:10.1029/2004GL019941.

Jian, L., C. T. Russell, J. G. Luhmann, and R. M. Skoug (2006), Properties of interplanetary coronal mass ejections at one AU during 1995–2004, *Sol. Phys.*, *239*, 393–436.

Kan, J. R., and L. C. Lee (1979), Energy coupling function and solar wind-magnetosphere dynamo, *Geophys. Res. Lett.*, *6*, 577–580.

Lepping, R. P., C.-C. Wu, and D. B. Berdichevsky (2005), Automatic identification of magnetic clouds and cloud-like regions at 1 AU: Occurrence rate and other properties, *Ann. Geophys.*, *23*, 2687–2704.

Lugaz, N., W. B. Manchester, and T. I. Gombosi (2005), Numerical simulation of the interaction of two coronal mass ejections from Sun to Earth, *Astrophys. J.*, *634*, 651–662.

Lugaz, N., W. B. Manchester, I. I. Roussev, G. Tóth, and T. I. Gombosi (2007), Numerical investigation of the homologous CME events from AR 9236, *Astrophys. J.*, *659*, 788–800.

Lugaz, N., C. J. Farrugia, J. A. Davies, C. Möstl, C. J. Davis, I. I. Roussev, and M. Temmer (2012), The deflection of the two interacting CMEs of 2010 May 23–24 as revealed by combined in situ measurements and HI, *Astrophys. J.*, *759*, 68.

Lugaz, N., C. J. Farrugia, W. B. Manchester, and N. Schwadron (2013), The interaction of two coronal mass ejections: Influence of relative orientation, *Astrophys. J.*, *778*, 20.

Manchester, W. B., T. I. Gombosi, I. Roussev, D. L. De Zeeuw, I. V. Sokolov, K. G. Powell, G. Tóth, and M. Opher (2004), Three-dimensional MHD simulation of a flux rope driven CME, *J. Geophys. Res.*, *109*, A01102, doi:10.1029/2002JA009672.

Marubashi, K., and R. P. Lepping (2007), Long-duration magnetic clouds: A comparison of analyses using torus- and cylinder-shaped flux rope models, *Ann. Geophys.*, *25*, 2453–2477.

Richardson, I. G., and H. V. Cane (2010), Near-Earth interplanetary CMEs during Solar Cycle 23 (1996–2009): Catalog and summary of properties, *Sol. Phys.*, *264*, 189–237.

Richardson, I. G., and J. Zhang (2008), Multiple-step geomagnetic storms and their interplanetary drivers, *Geophys. Res. Lett.*, *35*, L06S07, doi:10.1029/2007GL032025.

Richardson, I. G., E. W. Cliver, and H. V. Cane (2001), Sources of geomagnetic storms for solar minimum and maximum conditions during 1972–2000, *Geophys. Res. Lett.*, *28*, 2569–2572.

Rouillard, A. P., B. Lavraud, N. R. Sheeley, J. A. Davies, L. F. Burlaga, N. P. Savani, C. Jacquey, and R. J. Forsyth (2010), White light and in situ comparison of a forming merged interaction region, *Astrophys. J.*, *719*, 1385–1392.

Savani, N. P., M. J. Owens, A. P. Rouillard, R. J. Forsyth, and J. A. Davies (2010), Observational evidence of a coronal mass ejection distortion directly attributable to a structured solar wind, *Astrophys. J. Lett.*, *714*, L128–L132.

Shen, C., Y. Wang, S. Wang, Y. Liu, R. Liu, A. Vourlidas, B. Miao, P. Ye, J. Liu, and Z. Zhou (2012), Super-elastic collision of large-scale magnetized plasmoids in the heliosphere, *Nat. Phys.*, *8*, 923–928.

Shen, F., X. S. Feng, Y. Wang, S. T. Wu, W. B. Song, J. P. Guo, and Y. F. Zhou (2011), Three-dimensional MHD simulation of two coronal mass ejections' propagation and interaction using a successive magnetized plasma blobs model, *J. Geophys. Res.*, *116*, A09103, doi:10.1029/2011JA016584.

Tóth, G., et al. (2012), Adaptive numerical algorithms in space weather modeling, *J. Comput. Phys.*, *231*, 870–903.

Troshichev, O., P. Stauning, K. Liou, and G. Reeves (2011), Saw-tooth substorms: Inconsistency of repetitive bay-like magnetic disturbances with behavior of aurora, *Adv. Space Res.*, *47*, 702–709.

van der Holst, B., W. B. Manchester, R. A. Frazin, A. M. Vásquez, G. Tóth, and T. I. Gombosi (2010), A data-driven, two-temperature solar wind model with Alfvén waves, *Astrophys. J.*, *725*, 1373–1383.

Wang, Y. M., P. Z. Ye, and S. Wang (2003), Multiple magnetic clouds: Several examples during March–April 2001, *J. Geophys. Res.*, *108*(A10), 1370, doi:10.1029/2003JA009850.

Xie, H., N. Gopalswamy, P. K. Manoharan, A. Lara, S. Yashiro, and S. Lepri (2006), Long-lived geomagnetic storms and coronal mass ejections, *J. Geophys. Res.*, *111*, A01103, doi:10.1029/2005JA011287.

Zurbuchen, T. H., and I. G. Richardson (2006), In-situ solar wind and magnetic field signatures of interplanetary coronal mass ejections, *Space Sci. Rev.*, *123*, 31–43.